International Computer Music Conference (ICMC'94), Sept. 12–17, 1994, Aarhus, Denmark

Digital Waveguide Modeling of Wind Instrument Bores Constructed of Truncated Cones

Vesa Välimäki and Matti Karjalainen

Helsinki University of Technology
Acoustics Laboratory
Otakaari 5A, FIN-02150 Espoo, Finland

and

CARTES
(Computer Arts Centre at Espoo)
Ahertajankuja 4, FIN-02100 Espoo, Finland

vpv@vipunen.hut.fi, matti_karjalainen@hut.fi

Abstract

This paper deals with waveguide simulation of acoustic tube systems that are constructed of conical tube sections. Digital reflection filters needed for modeling the scattering that occurs at a junction of conical tubes are presented. It is known that the reflection filter can be unstable in certain cases. However, the overall system is stable if it corresponds to a physically realizable system. Furthermore, a fractional delay waveguide model (FDWM), where the length of each conical tube section can be accurately adjusted, is introduced. The methods described in this paper are directly applicable to the waveguide synthesis of wind instruments.

1 Introduction

Digital waveguide modeling has proved to be the most efficient technique for sound synthesis by physical models [Smith, 1992]. A typical waveguide model is well suited to implementation by a signal processor or a workstation. This technique is readily applicable to simulation and synthesis of wind instruments (see, e.g., [Smith, 1987], [Välimäki *et al.*, 1992]) as well as string (e.g., [Karjalainen *et al.*, 1993], [Smith, 1993]) and some percussion instruments [Van Duyne and Smith, 1993]. An additional advantage of waveguide models is that they have an intuitive physical interpretation.

A distinctive feature of physical modeling—when compared with traditional synthesis techniques—is that the musical instrument to be synthesized has to be studied carefully before the model can be developed. Each instrument has to be examined separately. Fortunately, musical instruments of the same family (e.g., woodwinds) share certain properties that can be modeled in a similar way. The examination of the physics of the instrument deals mainly with the sound production mechanism and losses in its resonator part. Furthermore, an intuition on what are the essential properties of the sound has to be gained. The resources have to be aimed at careful modeling of properties that have the most significant effect on the perceived sound. Namely, it does not pay to model features that are not perceptually relevant. This is the major strategy for simplifying a physical model and for turning it into an efficient DSP algorithm.

Currently, the basic theory of waveguide synthesis covers methods for simulating linear one and two-dimensional resonators. The work on acoustic tubes has mainly concentrated on cylindrical tubes and tube systems made up of concatenation of cylindrical tube sections. One possible extension to former work is thus waveguide simulation of non-cylindrical tubes.

This paper addresses the simulation of acoustic tube systems that are constructed of conical tube sections. The basic idea of applying waveguide simulation to non-cylindrical tubes was presented by Smith [1991]. The motivation for our work is that several woodwind instruments, e.g., saxophones, oboes, and bassoons, have a conical bore. Conical tube sections can also be used for approximating other smoothly varying tube shapes, such as exponential horns that are needed in physical modeling of brass instruments. Formerly, non-cylindrical acoustic tubes have been approximated by short cylindrical tube sections (see, e.g., [Cook, 1988]). As the number of these sections is increased and their length decreased, the model gets more and more accurate. The computational load, however, is increased considerably at the same time.

The main contribution of the present work is the introduction of digital filters and structures for modeling conical tube systems. The results can be directly applied to the waveguide synthesis of wind instruments that have conical parts in their bore. We also demonstrate how the length of the conical sections can be modeled accurately by employing fractional delays (FDs). Such an extended model is called a *fractional delay waveguide model* (FDWM). The basic principles of FDWMs were presented in [Välimäki *et al.*, 1993*a*]. Our earlier work on FDWMs includes

simulation of finger holes in a cylindrical woodwind bore [Välimäki *et al.*, 1993*b*] and modeling of the human vocal tract [Välimäki *et al.*, 1994*a*] [Välimäki *et al.*, 1994*b*].

This paper is organized as follows. In Section 2, the wave propagation in a conical acoustic tube is discussed, and reflection functions and related digital filters needed in a conical tube simulation are introduced. The continuous-time approximations for the reflection functions have been derived by Martínez and Agulló [1988]. These functions are converted into digital filters by using the *impulse-invariant transformation*, which is a standard technique in signal processing. We review this method briefly in Appendix A.

Section 3 discusses discrete-time systems constructed of conical bores. An example shows that the waveguide approach leads to results similar to those reported earlier in the literature. Furthermore, it is shown that the scaling factors (associated with the spherical wave propagating in a conical tube) can be commuted and lumped at the output of the waveguide model.

In Section 4, the model is extended by incorporating fractional delays. The FD filtering techniques—especially *deinterpolation*—are shortly recapitulated and the use of FIR FD filters in waveguide modeling is discussed. Finally, Section 5 summarizes the results and gives directions for future work.

2 Theory of Conical Tubes

2.1 Wave Propagation in a Conical Acoustic Tube

Propagation of acoustic waves can be described by the wave equation. The linear wave equation for a spherical pressure wave traveling in a conical bore is a second-order partial differential equation given by (see, e.g., [Ayers *et al.*, 1985] or [Smith, 1991])

$$\frac{\partial^2 \psi(r,t)}{\partial t^2} = c^2 \frac{\partial^2 \psi(r,t)}{\partial r^2} \tag{1}$$

where c is the speed of sound, r is the distance from the tip of the cone and $\psi(r,t)$ is defined by

$$\psi(r,t) = rp(r,t) \tag{2}$$

where p denotes the acoustic pressure. The well-known traveling wave solution for Eq. (1) is of the form

$$p(r,t) = \frac{f(t-\frac{r}{c})}{r} + \frac{g(t+\frac{r}{c})}{r} \tag{3}$$

where $f(t-\frac{r}{c})$ and $g(t+\frac{r}{c})$ are the components of the spherical wave that travel in the positive and negative r-direction, respectively.

The traveling wave solution given by Eq. (3) can be sampled to obtain the form suitable for digital simulation [Smith, 1991]. Thus we can define

$$p^+(n) = f(nT-\tfrac{r}{c}) \quad \text{and} \quad p^-(n) = g(nT+\tfrac{r}{c}) \tag{4}$$

The total pressure $p(n)$ at point r is then obtained as

$$p(n,r) = \frac{1}{r}\Big[p^+(n) + p^-(n)\Big] \tag{5}$$

The implementation of an output in a digital waveguide representing a conical tube requires the computation of a division (by r) per output sample. This is typically a computationally expensive operation in a signal processor implementation. If the location of the output is constant or there is a finite number of output points, it is recommendable to store the desired values $\rho = 1/r$ in a table and then use the proper value as a multiplier.

2.2 Reflection Function for a Junction of Conical Sections

The acoustic pressure wave traveling in a conical tube is disturbed by any abrupt change of diameter or taper. The reflection and transmission phenomena are clearly illustrated in [Martínez *et al.*, 1988]. The reflection function for a pressure wave at the junction of two tube sections with differing taper and diameter is given by [Martínez and Agulló, 1988][†]

$$R_c(\omega) = \frac{B-1}{B+1} - \frac{2B\alpha}{(B+1)(j\omega+\alpha)} \tag{6}$$

where the subscript 'c' denotes 'continuous-time' and α is defined by

$$\alpha = -\frac{c}{A_a + A_b}\left(\frac{A_a}{r_a} - \frac{A_b}{r_b}\right) \tag{7}$$

where c is the speed of sound, and B is the area ratio of the sections a and b at the joint, i.e.,

$$B = \frac{A_a}{A_b} \tag{8}$$

The transmission function $T_c(\omega)$ that determines the signal that propagates through the junction is defined by

$$T_c(\omega) = 1 + R_c(\omega) \tag{9}$$

Note that in limit $r_a, r_b \to \infty$ the reflection function given by Eq. (6) approaches the reflection coefficient for a junction of two cylindrical tubes.

[†] The notation used here is not the same as that used by Martínez and Agulló [1988], but instead we have adopted it from [Gilbert *et al.*, 1990].

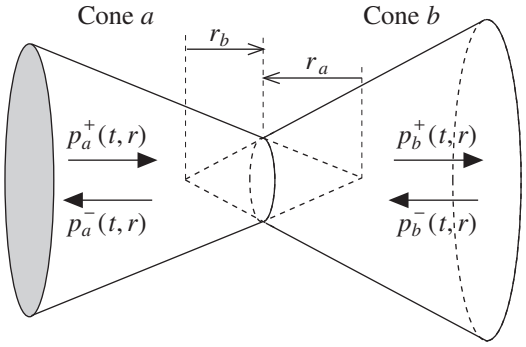

Fig. 1 A *junction of conical tubes that have the same diameter at the joint. In this example* $r_a < 0$ *and* $r_b > 0$.

A digital filter approximating the reflection function is obtained by impulse-invariant transforming Eq. (6). This yields

$$R(z) = \frac{B-1}{B+1} - \frac{2BT\alpha/(B+1)}{1-e^{-\alpha T}z^{-1}} \qquad (10)$$

This is a first-order filter with one real pole.

2.3 Reflection Function With Taper Discontinuity Only

A useful special case of Eq. (6) is obtained setting the areas A_a and A_b equal. This implies that $B = 1$. Substituting this into Eq. (6) we obtain the reflection function for a junction with taper discontinuity only (see Fig. 1). The reflection function is then simply

$$R_c(\omega) = -\frac{\alpha}{\alpha + j\omega} \qquad (11)$$

where the coefficient α is now given by

$$\alpha = -\frac{c}{2r_a} + \frac{c}{2r_b} = \frac{c(r_a - r_b)}{2r_a r_b} \qquad (12)$$

where c is the speed of sound and r_a and r_b are the distances from the (imagined) tips of cones a and b, respectively, as illustrated in Fig. 1.

The impulse-invariant transform of this function yields a first-order all-pole filter

$$R(z) = \frac{b_0}{1 + a_1 z^{-1}} \qquad (13)$$

with the filter coefficient $a_1 = -e^{-\alpha T}$ where α is defined as in Eq. (12). It is necessary to scale this transfer function to have unity gain at $\omega = 0$. This is achieved by setting $b_0 = -(1 + a_1)$.

Figure 2 shows the magnitude responses $|R_c(\omega)|$ and $|R(e^{j\omega})|$ with five different values of r_b. The parameter r_a is equal to 0.1 m in these examples. The effect of aliasing due to the impulse-invariant transformation is clearly seen by comparing the curves of the analog (dotted lines) and the digital (solid lines) filters. Note, however, that the difference

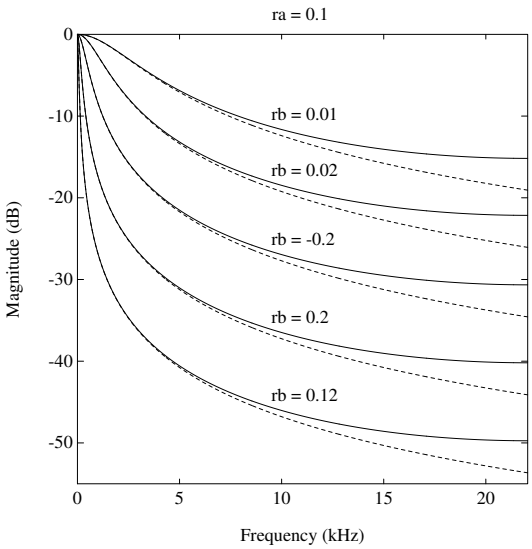

Fig. 2 *Magnitude responses of the analog (dashed lines) and digital (solid lines) reflection functions with taper discontinuity only. The sampling rate is 44.1 kHz.*

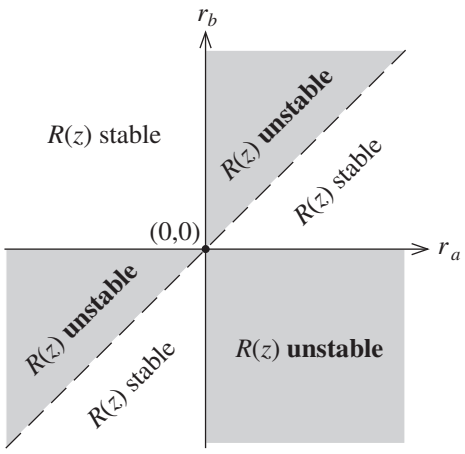

Fig. 3 *The stability of the reflection filter R(z) depends on the parameters* r_a *and* r_b. *The filter is unstable in the shaded regions.*

between the magnitude response pairs is several dBs only at frequencies over 10 kHz. At low frequencies, which are of great importance, the digital approximations coincide with the analog ones.

Above we have considered the reflection from the positive side of a junction, that is, $R(z) = R^+(z)$. The reflection function $R^-(z)$ from the negative direction is the same as the one from the positive direction. This is observed by considering the mirror image of a junction. Then the value for r_a is replaced with $-r_b$ and r_b with $-r_a$. By substituting these values into Eq. (13) it is seen that

$$\alpha' = \frac{c\left[-r_b - (-r_a)\right]}{2(-r_b)(-r_a)} = \frac{c(r_a - r_b)}{2r_a r_b} = \alpha \qquad (14)$$

and thus $R^-(z) = R^+(z) = R(z)$ when $A_a = A_b$.

2.4 Stability of the Reflection Filter

The reflection filter $R(z)$ defined by Eq. (13) is stable when its pole (i.e., root of the denominator of the transfer function) lies inside the unit circle in the complex plane, that is, $|p| < 1$. This is equivalent to the requirement that $e^{-\alpha T} < 1$ which consequently implies that α must be positive (since $T > 0$). Finally, the sign of α depends on the values of r_a and r_b according to Eq. (12).

The regions of stability and unstability of $R(z)$ are illustrated in Fig. 3 on a parameter plane where the abscissa corresponds to the value of r_a and the ordinate to the value of r_b. There are three distinct regions where the filter $R(z)$ is stable and three where it is unstable. The unstable regions include half of all possible conical tube configurations. These cases may be impossible to avoid in practice.

Fortunately it appears that having an unstable filter as a part of a larger system does not necessarily imply that the overall system is unstable. Physical systems are passive and they are always stable. Also digital models that simulate physically realizable systems have to be stable.

2.5 Closed End of a Conical Tube

When the end of a truncated conical tube is closed, the radiation impedance $Z(\omega)$ tends to infinity. Then the reflection function of a spherical wave is written as [Martínez and Agulló, 1988]

$$R_c(\omega) = \lim_{Z(\omega)\to\infty} \frac{Z(\omega)\left(j\omega + \frac{c}{r_e}\right) - Z_0}{Z(\omega)\left(j\omega - \frac{c}{r_e}\right) + Z_0} = \frac{j\omega + \frac{c}{r_e}}{j\omega - \frac{c}{r_e}} = 1 + \frac{2\frac{c}{r_e}}{j\omega - \frac{c}{r_e}} \tag{15}$$

where $Z_0 = \rho c$ is the characteristic impedance.

The impulse-invariant transform of the last form yields

$$R(z) = 1 + \frac{b_0}{1 + a_1 z^{-1}} \tag{16}$$

with the coefficients $b_0 = 2cT / r_e$ and $a_1 = -e^{cT/r_e}$. This transfer function is stable when $r_e < 0$ but unstable when $r_e > 0$. For $r_e = 0$ Eq. (16) is not well defined. This is not a problem in practice because the case is not physically meaningful. Note that in the limit $r_e \to \infty$ the transfer function approaches unity, which is the reflection coefficient for a closed end of a lossless cylindrical tube.

2.6 Open End of a Conical Tube

The acoustic impedance of an open end of a conical tube has not been theoretically formulated. Thus it is not possible to derive the analytic form of the corresponding reflection function. As a first approximation we use the *ad hoc* continuous-time reflection function proposed by Martínez [Martínez and Agulló, 1988]:

$$r_c(t) = \begin{cases} -a^2 t e^{-at} & t \ge 0 \\ 0 & t < 0 \end{cases} \tag{17}$$

with

$$a = c\left(\frac{0.787e}{D} - \frac{1}{2r_e}\right) \tag{18}$$

where c is the speed of sound, D is the diameter of the open end, r_e the distance of the opening from the apex of the conical tube section, and $e \approx 2.71828$.

Equation (17) is easily transformed into the frequency domain employing the well-known property that multiplication by t in the time domain corresponds to differentiation with respect to the frequency variable in the frequency domain. Thus, the Laplace transform of Eq. (17) can be written as

$$R_c(s) = -a^2 \frac{d}{ds}\left(\frac{1}{s+a}\right) = -\frac{a^3}{(s+a)^2} \tag{19}$$

The corresponding z-transform obtained using the impulse-invariant method is given by

$$R(z) = -a^2 \frac{d}{dz}\left(\frac{1}{1 - e^{-aT} z^{-1}}\right) \tag{20}$$

This yields

$$R(z) = \frac{b_1 z^{-1}}{1 + a_1 z^{-1} + a_2 z^{-2}} \tag{21}$$

with the coefficients

$$b_1 = -a^2 T^2 e^{-aT},\ a_1 = -2e^{-aT},\ a_2 = e^{-2aT} \tag{22}$$

The impulse response of the digital filter given by Eq. (21) is a sampled version of Eq. (17), that is,

$$r(n) = -a^2 nTe^{-anT} \text{ for } n = 0, 1, 2\text{K} \tag{23}$$

This reflection function is not an accurate approximation as is easily noticed by comparing the impulse responses shown in [Martínez and Agulló, 1988]. A higher-order transfer function would be needed to account for the behavior that is seen in the figures on page 1617 in [Martínez and Agulló, 1988].

The function given by Martínez and Agulló approximates the reflection of a pressure wave from

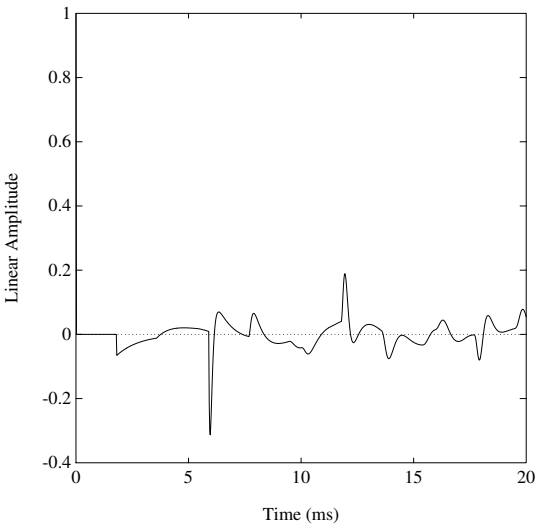

Fig. 4 *Impulse response of a tube system constructed of a cylindrical and a conical tube. This result may be compared to that given by [Martínez et al., 1988].*

the open end of a conical tube in an infinite wall. Note that this case is not of interest in modeling wind instruments. Rather, we should find a proper approximation for the situation where there is no wall of any kind, but the tube is in free space.

A first-order approximation for the radiation impedance of the open end of a conical tube is obtained using the impedance of a spherical source of an equivalent radiation area. Interestingly enough this impedance has the same form as that of an infinite conical section.

3 Digital Waveguide Model for a Conical Tube System

In this section we study complete waveguide systems that simulate conical tubes. We only discuss systems where the joint of conical tubes does not have a discontinuity in diameter (see Sec. 2.3). Then the reflection function $R(z)$ is the same in both directions.

3.1 Numerical Example

As a simple example we simulate the bore described on page 1623 in [Martínez *et al.*, 1988]. This system consists of two pieces, a cylindrical tube (length 300 mm) and a conical tube (length 700 mm). One end of the system is closed (diameter 10 mm) and the other is open (diameter 50 mm). A unit impulse is fed from the closed end of the cylindrical tube and the response is registered at the same point. The sampling rate is 44.1 kHz.

Figure 4 illustrates the first 20 ms of the impulse response. This result can be compared with Figs. 8a and 8b of [Martínez *et al.*, 1988]. In our simulation losses have not been included while Martínez *et al.* had incorporated frequency-dependent losses. Most of the losses are obviously due to the open-end reflection function discussed in section 2.6. It is seen that the impulse response obtained by the waveguide simulation (Fig. 4) is very similar to those presented in the reference. Their results were obtained using multiconvolution and discrete Fourier transform.

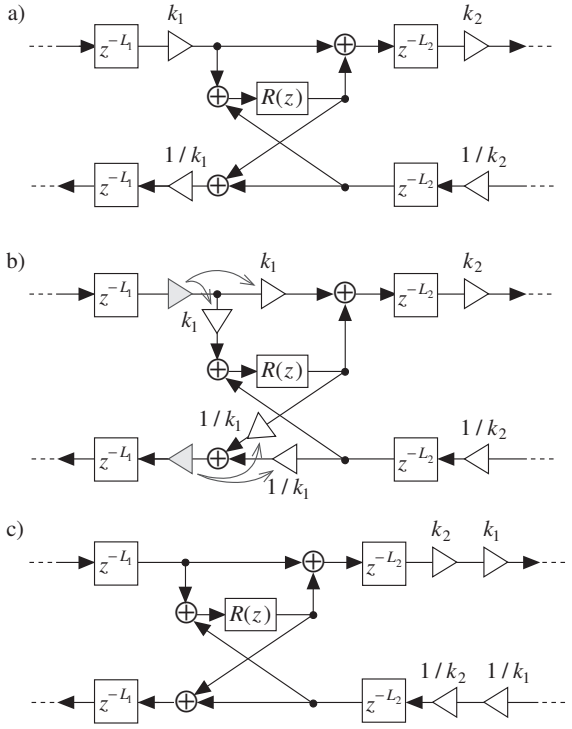

Fig. 5 *The scaling factors associated with the conical waveguide sections can be commute. Thus they can be pushed through the scattering junctions.*

3.2 Commuting the Scaling Factors

In Section 2.1 we discussed the wave propagation in a conical tube. It was mentioned that a division is needed to scale the pressure according to the position along the tube. Let us consider a waveguide model constructed of two conical section (see Fig. 5). The scaling factors k_1 and k_2 are defined as follows:

$$k_1 = \frac{r_1}{r_1 - l_1} \quad \text{and} \quad k_2 = \frac{r_2}{r_2 - l_2} \tag{24}$$

where r_1 and r_2 are the distances from the tips of the cones 1 and 2, respectively, and l_1 and l_2 are the lengths (in meters) of the corresponding cones.

If the value of the pressure signal is not needed to observe at any point inside a waveguide system, the scaling factors can be commuted so that they are all computed at the input or the output of the system. Figure 5 illustrates how k_1 is pushed through the scattering junction by placing a copy of it to each signal path after a node. The factor $1/k_1$ of the lower delay line can be commuted in a similar manner.

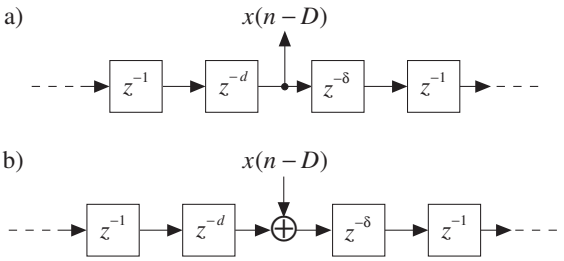

Fig. 6 *a) Output and b) input at a fractional point of a digital delay line.*

4 Fractional Delay Waveguide Model

This section discusses the application of *fractional delays* (FDs) to the modeling of conical tubes. The need for FDs is obvious when the length of the tube to be simulated does not correspond to an integral multiple of the sampling interval. In addition, FDs are essential in the simulation of finger holes, whose position on the bore determines the pitch [Välimäki *et al.*, 1993*b*].

Note, however, that it is not necessary to use FDs in the simulation where a non-uniform tube profiles, e.g., that of the horn of a trumpet, is modeled concatenating short conical tubes sections. Then it is adequate that the lengths of the sections correspond to the unit delay or its multiple.

4.1 Interpolation vs. Deinterpolation

In a typical FD application, the problem to be solved is to estimate the value of a discrete-time signal at an arbitrary location between the known samples. This can equivalently be stated as locating an *output* point to a digital delay line (see Fig. 6a).

In a physical model for wave propagation, it is often needed to add a signal to an arbitrary point of a delay line. This is equivalent to having an *input* point in the middle of a digital delay line as illustrated in Fig. 6b. This idea has helped to develop more intuitive and easily controllable physical models.

In Fig. 6, the block labeled by z^{-d} represents an ideal fractional delay of d ($0 \le d < 1$). The corresponding frequency response is obtained setting $z = e^{j\omega}$. This yields

$$H(e^{j\omega}) = e^{-j\omega d} \tag{25}$$

where $j = \sqrt{-1}$ and ω is the radial frequency in rad. Here the sampling rate has been normalized to 1 and thus the sampling interval T is also 1.

The variable δ is called the *complementary fractional delay* and it is defined by

$$\delta = 1 - d \tag{26}$$

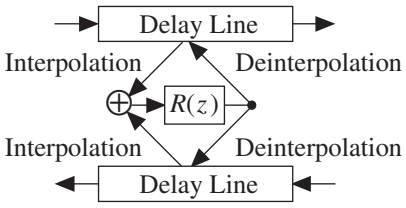

Fig. 7 *The interpolated scattering junction. The input signal of $R(z)$ is obtained as a sum of signals that are interpolated from the delay lines. The output signal is superimposed onto both delay lines by deinterpolation.*

Together the fractional delay elements z^{-d} and $z^{-\delta}$ construct a unit delay, that is

$$z^{-d} z^{-\delta} = z^{-(d+\delta)} = z^{-1} \tag{27}$$

The system of Fig. 6a requires the use of a well-known numerical technique, interpolation. The operation used in Fig. 6b to add a signal "between the samples of a delay line" is an inverse operation of interpolation. This operation has been given the name *deinterpolation*† [Välimäki *et al.*, 1993*a*].

The major difference between interpolation and the corresponding deinterpolation is that the former realizes a fractional delay d while the latter the complementary delay δ. This is seen by considering Fig. 6 again: in interpolation the outgoing signal $x(n–D)$ travels through the element z^{-d} (see Fig. 6a) and in deinterpolation the ingoing signal $x(n–D)$ goes through $z^{-\delta}$ (see Fig. 6b).

Interpolation can be implemented using the standard direct-form FIR filter structure. Deinterpolation can be implemented by the *transpose FIR filter structure*. Note that the coefficients $h(n)$ of the deinterpolator must be in the time-reversed order with respect to the transpose FIR filter structure since the deinterpolator approximates the complementary delay $z^{-\delta}$. The implementation of interpolation and deinterpolation by FIR filter structures is discussed in [Välimäki *et al.*, 1993*a*] and [Välimäki *et al.*, 1993*b*].

4.2 The Conical FDWM

The conical fractional delay waveguide model (FDWM) is constructed by replacing each scattering junction with an interpolated one that is depicted in Fig. 7. The input of the reflection function $R(z)$ is obtained as a sum of the interpolated signal values from both delay lines. Its output is superimposed onto the delay lines using deinterpolation, which can be implemented by the transpose FIR filter structure as explained earlier.

A complete FDWM consists of an arbitrary number of interpolated scattering junctions. The location

† A more obvious name 'inverse interpolation' cannot be used, because it is reserved for other use in mathematics. Thus, a new word had to be invented.

of each junction can be adjusted by computing the proper coefficients in the FIR interpolation and deinterpolation filters. A time-varying conical tube model can be implemented by changing the filter coefficients as a function of time. The FIR FD filters do not cause disturbing transients if the changes of the interpolation point are not large. This technique may also be used for modeling the human vocal tract [Välimäki and Karjalainen, 1994].

5 Summary and Future Work

This paper has introduced a method for efficient simulation of conical tubes. Digital filters that approximate the continuous-time reflection functions have been presented. The use of fractional delay techniques enables accurate control of the length of the conical tube sections in the model. We are applying these technique also to the modeling of the human vocal tract. The first results will be presented in a forth-coming paper [Välimäki and Karjalainen, 1994].

The waveguide simulation of acoustic tubes constructed of conical parts is a new area of research. Several questions are left for future research. For example, waveguide simulation of finger holes in conical bore should be studied using the formulations given in [Martínez *et al.*, 1988]. This is essential for the modeling of woodwind instruments such as the saxophone. Furthermore, the stability of the overall waveguide model is an issue that should be demonstrated in the general case or at least for certain useful configurations.

Another important topic for future research is to verify the accuracy of the digital model by acoustic measurements. Tube systems including conical parts can be excited by a short pulse and the response measured by a microphone. The actual impulse response is then obtained by deconvolution of the pulse and the response. These results may be compared to those obtained using a waveguide model. Agulló *et al.* [1993] have measured conical tube systems and showed that the results are in good agreement with the theoretical formulations reported in [Martínez and Agulló, 1988].

A major unsolved problem is the reflection function for the open end of a conical tube. The exact mathematical solution is obviously involved. Hence we suggest a series of measurements of impulse responses and reflection functions of open conical horns of different taper and diameter. A useful digital reflection filter may then be designed applying one of the standard techniques used in digital signal processing.

Appendix A. Impulse-Invariant Transformation

The impulse-invariant transformation is a technique for converting an analog system into a digital one (see, e.g., [Jackson, 1986, pp. 198–200] or [Parks and Burrus, 1987, pp. 206–209]). This method preserves the impulse response (IR) of the analog system, that is

$$h(n) = T\, h_c(nT) \tag{A1}$$

where $h(n)$ is the IR sequence of the discrete-time system, $h_c(t)$ is the IR of the original continuous-time system, and T is the sampling interval or one over the sample rate. In other words, the IR of the analog system is sampled and the samples are used as the IR of the digital filter. The IR is scaled by T to keep the maximum gain comparable to that of the analog system.

In practice, the impulse-invariant transformation is not performed for the impulse response but for the transfer function. First, the analog transfer function has to be written as a sum of all-pole subsystems:

$$H_c(\omega) = \sum_{k=1}^{N} \frac{jA_k}{\omega - \omega_k} \tag{A2}$$

where $j = \sqrt{-1}$, N is the order of the system (i.e., number of poles), ω is the radial frequency (rad), and ω_k are the poles of the transfer function. The transfer function of a discrete-time system with the same impulse response is then expressed as

$$H(z) = \sum_{k=1}^{N} \frac{A_k T}{1 - e^{j\omega_k T} z^{-1}} \tag{A3}$$

The frequency response of the filter will, however, not be preserved by the impulse-invariant transformation. The frequency response of the digital system can be written by means of the desired analog response as

$$H(\omega) = \sum_{k=-\infty}^{\infty} H_c\left[j\left(\omega - \frac{2\pi k}{T} \right) \right] \tag{A4}$$

This is an *aliased* version of the analog frequency response. Due to this the method is not applicable to analog highpass filters. Fortunately, physical systems that we are concerned with in this paper have usually a lowpass transfer function.

Although the aliasing distorts the frequency response at high frequencies it does not make the approximations useless since it is more important to have accurate approximation at low frequencies. The effect of aliasing on lowpass magnitude responses can be observed in Fig. 2.

Acknowledgment

This work was financed by the Academy of Finland.

References

[Ayers *et al.*, 1985] R. Dean Ayers, Lowell J. Eliason, and Daniel Mahgerefteh. The conical bore in musical acoustics. *Am. J. Phys.*, **53** (6): pp. 528–537, June 1985.

[Agulló *et al.*, 1993] J. Agulló, S. Cardona, and D. H. Keefe. Time-domain measurements of reflection functions for discontinuities in wind-instrument air columns. In *Proc. Stockholm Music Acoustics Conf. (SMAC 93)*, Stockholm, Sweden, July 28–Aug. 1, 1993, to be published.

[Cook, 1988] Perry R. Cook. Implementation of single reed instruments with arbitrary bore shapes using digital waveguide filters. Stanford, CA, Stanford University, Dept. of Music, CCRMA, Tech. Report No. STAN–M–50, May 1988.

[Gilbert *et al.*, 1990] J. Gilbert, J. Kergomard, and J. D. Pollack. On the reflection functions associated with discontinuities in conical bores. *J. Acoust. Soc. Am.*, **87** (4): pp. 1773–1780, April 1990.

[Jackson, 1989] Leland B. Jackson. *Digital Filters and Signal Processing. Second Edition*, Kluwer, Boston, 1989.

[Karjalainen *et al.*, 1993] Matti Karjalainen, Vesa Välimäki, and Zoltán Jánosy. Towards high-quality sound synthesis of the guitar and string instruments. In *Proc. ICMC'93*, Tokyo, Japan, pp. 56–63, Sept. 10–15, 1993.

[Martínez and Agulló, 1988] J. Martínez and J. Agulló. Conical bores. Part I: Reflection functions associated with discontinuities. *J. Acoust. Soc. Am.*, **84** (5): pp. 1613–1619, Nov. 1988.

[Martínez *et al.*, 1988] J. Martínez, J. Agulló, and S. Cardona. Conical bores. Part II: Multiconvolution. *J. Acoust. Soc. Am.*, **84** (5): pp. 1620–1627, Nov. 1988.

[Parks and Burrus, 1987] T. W. Parks and C. S. Burrus. *Digital Filter Design*, Wiley, New York, pp. 206–209, 1987.

[Smith, 1987] Julius O. Smith. *Music Applications of Digital Waveguides*. Stanford, CA, Stanford University, Dept. of Music, CCRMA, Report No. STAN–M–39, May 27, 1987.

[Smith, 1991] Julius O. Smith. Waveguide simulation of non-cylindrical acoustic tubes. In *Proc. ICMC'91*, Montreal, Canada, pp. 304–307, Oct. 16–20, 1991.

[Smith, 1992] Julius O. Smith. Physical modeling using digital waveguides. *Computer Music J.*, **16** (4): pp. 75–87, Winter 1992.

[Smith, 1993] Julius O. Smith. Efficient synthesis of stringed musical instruments. In *Proc. ICMC '93*, Tokyo, pp. 64–71, Sept. 10–15, 1993.

[Välimäki *et al.*, 1992] Vesa Välimäki, Matti Karjalainen, Zoltán Jánosy, and Unto K. Laine. A real-time DSP implementation of a flute model. In *Proc. 1992 IEEE Int. Conf. Acoust., Speech, and Signal Process. (ICASSP'92)*, San Francisco, CA, vol. II, pp. 249–252, March 23–26, 1992.

[Välimäki *et al.*, 1993*a*] Vesa Välimäki, Matti Karjalainen, and Timo I. Laakso. Fractional delay digital filters. In *Proc. 1993 IEEE Int. Symp. Circuits and Systems (ISCAS'93)*, Chicago, IL, vol. 1, pp. 355–358, May 3–6, 1993.

[Välimäki *et al.*, 1993*b*] Vesa Välimäki, Matti Karjalainen, and Timo I. Laakso. Modeling of woodwind bores with finger holes. In *Proc. ICMC'93*, Tokyo, Japan, pp. 32–39, Sept. 10–15, 1993.

[Välimäki *et al.*, 1994*a*] Vesa Välimäki, Matti Karjalainen, and Timo Kuisma. Articulatory control of a vocal tract model based on fractional delay waveguide filters. In *Proc. 1994 IEEE Int. Symp. Speech, Image Processing and Neural Networks (ISSIPNN'94)*, Hong Kong, vol. 2, pp. 585–588, April 13–16, 1994.

[Välimäki *et al.*, 1994*b*] Vesa Välimäki, Matti Karjalainen, and Timo Kuisma. Articulatory speech synthesis based on fractional delay waveguide filters. In *Proc. 1994 IEEE Int. Conf. Acoust., Speech, Signal Process. (ICASSP'94)*, Adelaide, Australia, vol. 1, pp. 571–574, April 19–22, 1994.

[Välimäki and Karjalainen, 1994] Vesa Välimäki and Matti Karjalainen. Improving the Kelly–Lochbaum vocal tract model using conical tube sections and fractional delay filtering techniques. In *Proc. 1994 Int. Conf. on Spoken Language Processing (ICSLP'94)*, Yokohama, Japan, Sept. 18–22, 1994, to be published.

[Van Duyne and Smith, 1993] Scott A. Van Duyne and Julius O. Smith. Physical modeling with the 2-D digital waveguide mesh. In *Proc. ICMC'93*, Tokyo, Japan, pp. 40–47, Sept. 10–15, 1993.